

1 *Supporting information of*

2 **Dynamical heterogeneity in the gelation process of a polymer solution with a lower critical**

3 **solution temperature**

4 Yingkang Dai<sup>†</sup>, Runlin Zhang<sup>†</sup>, Weixiang Sun<sup>†‡\*</sup>, Tao Wang<sup>†‡</sup>, Yunhua Chen<sup>†</sup>, Zhen Tong<sup>†</sup>

5

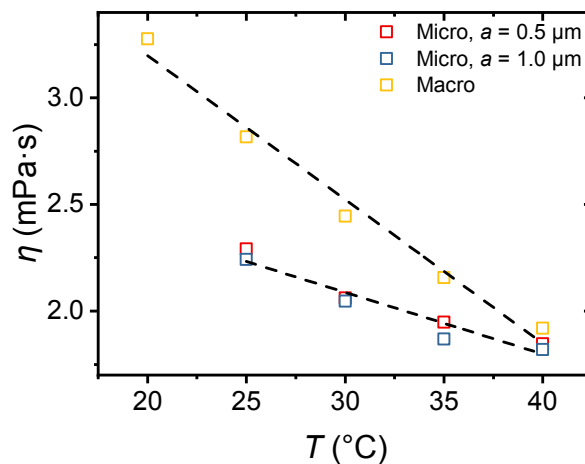
## 6 1. Temperature calibration of the microrheology

### 7 1.1 Methods

8 The temperature of the sample  $T$  under microrheological observation differed significantly  
9 from the nominal values of the incubator  $T_{\text{nominal}}$ . The viscosity–temperature dependence of a  
10 glycerol/water mixture was measured under a rotational rheometer (ARES-RFS, TA Instruments).  
11 Viscosity of the same sample was also measured by microrheology at a series of nominal incubator  
12 temperatures. The sample temperature  $T$  is believed to be the same as  $T_{\text{ARES}}$  when the two viscosities  
13 equal each other. The temperature of microrheology was then calibrated using the temperature of  
14 ARES-G2.

### 15 1.2 Results

16 As shown in Figure S 1 the measured viscosities from both microrheology and  
17 macrorheology depends on the nominal temperature of the corresponding instruments linearly with  
18 different slopes. By equating the two viscosity, the nominal temperatures from the two instruments  
19 have the relation  $T_{\text{micro}} = 23.6 \text{ }^\circ\text{C} + 0.43 T_{\text{macro}}$ .



20

21 Figure S 1 Viscosities of microrheology by two sizes of probe particles ( $a = 0.5 \text{ } \mu\text{m}$  and  $1.0 \text{ } \mu\text{m}$ )  
22 plotted against the nominal temperature of the incubator; Viscosity of macrorheology plotted against  
23 the rheometer temperature. Dash: linear fit.

## 24 **2. Static error measurement**

### 25 *2.1 Methods*

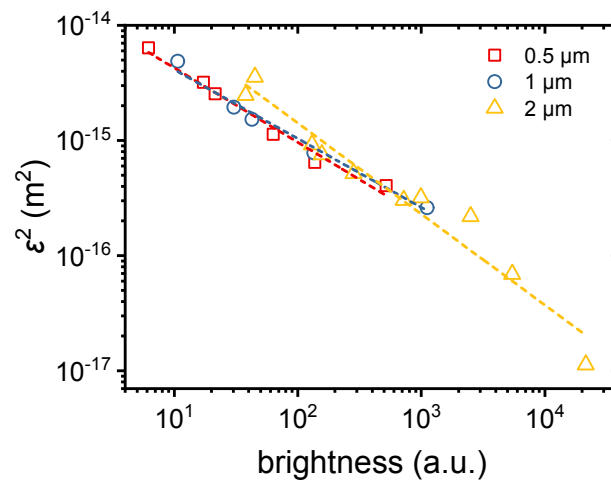
26 Synthetic hectorite (LAPONITE® XLG, BYK Rockwood Ltd.) was dried in vacuum at 50 °C  
27 for 12 hr. The dried powder of the clay was then gradually added to deionized water during stirring  
28 to ensure no large agglomeration occur. After the addition of clay, the suspension was stirred for 10  
29 min and ultrasonicated for 5 min. NaCl solution was then added to the suspension and stirred for 5  
30 min. The container of the suspension was then sealed with paraffin. In this experiment, the  
31 concentration of the clay  $c_L$  is 3%wt and the concentration of NaCl  $c_s$  is 1 mM. During the  
32 preparation of hectorite suspension, carboxylate-modified fluorescent polystyrene microspheres of  
33 diameter  $2a = 0.5 \mu\text{m}$ ,  $1 \mu\text{m}$  and  $2 \mu\text{m}$  dispersion of 2% solids content (FluoSphere®, ThermoFisher)  
34 were diluted with deionized water to particle concentration of 0.02%wt, 0.04%wt and 0.08%wt,  
35 respectively. After the hectorite is dissolved totally, the prepared microsphere dispersion was added  
36 to the solution to a final particle concentration of 0.0002% wt, 0.0004%wt and 0.0008%wt,  
37 respectively. The mixed solution was injected into a home-made glass chamber sealed with vacuum  
38 grease for microscopic observations. After 3 hours, the hectorite suspension L<sub>3</sub>S<sub>1</sub> had finished the  
39 gelation, it is a colloidal hydrogel with a modulus of *ca.* 100 Pa. Therefore, probe particles are  
40 effectively immobile within the time scale and resolution of our microrheology observation. The  
41 “tracks” identified by our routines are the static error, denoted as  $\varepsilon^2$ .

42 The trajectories of the probe particles in the Hectorite hydrogel were recorded under a  
43 fluorescent inverted microscope (Nikon Eclipse Ti-s) with a 60x oil-immersed objective of numerical  
44 aperture (NA) of 1.40. The brightness of the probe particles was varied by adding neutral density  
45 filter to the exciting beam. The field of view (FOV) was set to be  $276.48 \mu\text{m} \times 233.28 \mu\text{m}$   
46 approximately. The sample temperature was  $30 \pm 0.1 \text{ }^\circ\text{C}$ . Videos were acquired at 49.65 frame per  
47 second (fps) and 0.01 ms exposure time using an sCMOS camera (Zyla, Andor) at resolution  $2560\text{px}$   
48  $\times 2160\text{px}$ , corresponding to the pixel size of  $0.108 \mu\text{m}$  per px. Typically, around 50 in-frame

49 particles were tracked The trajectories of the particles were extracted by a MATLAB routine  
 50 modified based on the one by Blair and Dufresne.<sup>1</sup>

## 51 2.2 Result

52 We found that the static error of the particles depends only on the brightness, as shown in  
 53 Figure S 2, since the data of different sizes of probe particles collapse into one master curve when  
 54 plotted this way. The data of different sizes of probe particle do not collapse into one master curve  
 55 when plotted against signal-noise ratio (SNR). We therefore constructed working curves by linear  
 56 fitting the data and estimate the static error according to the brightness in each experiment.



57  
 58 Figure S 2 Static error plotted against the brightness of the probe particles.

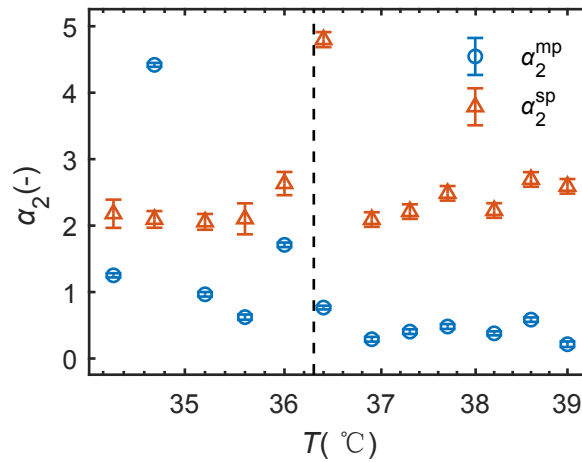
## 59 3. The standard error of the non-Gaussian paramete

60 The kurtosis  $g_2$  of  $N$  independent and identically distributed random variables  $x_i, i = 1, \dots, N$  is  
 61 subjected to small sample bias which lead to standard error depending on the value of  $N$  by the  
 62 following relation<sup>2</sup>

$$63 \quad \text{Var}(g_2) = \frac{24N(N-2)(N-3)}{(N+1)^2(N+3)(N+5)}$$

64 The non-Gaussian parameter  $\alpha_2 = g_2/3$ . The standard error of the non-Gaussian parameters was  
 65 shown in Figure S 3 for two typical lag times in the form of error bars. The variation of non-

66 Gaussian parameter versus temperature is highly significant compared with the error bars, which  
67 means the number of samples  $N$  in the present study are generally high enough for meaningful  
68 distussion of the non-Gaussian parameteres.



69  
70 Figure S 3 Circles: multi-particle non-Gaussian parameters at  $\Delta t = 0.24$  s; Triangles: single-particle  
71 non-Gaussian parameters at  $\Delta t = 14.9$  s.

72

### 73 Reference

74 1. Blair, D.; Dufresne, E., The matlab particle tracking code repository. *Particle-tracking code*  
75 available at <http://physics.georgetown.edu/matlab> 2008.

76 2. Cramér, H., *Mathematical Methods of Statistics*. Princeton University Press: 1999.

77